Air Composition over the Russian Arctic: 3u2014Trace Gases

O. Yu Antokhina, P. N. Antokhin, V. G. Arshinova, M. Yu Arshinov, B. D. Belan, S. B. Belan, D. K. Davydov, G. A. Ivlev, A. V. Kozlov, T. M. Rasskazchikova, et al.

ISSN 1024-8560, Atmospheric and Oceanic Optics, 2024, Vol. 37, No. 1, pp. 31–47. © The Author(s), 2024. This article is an open access publication, corrected publication 2024.
Russian Text © The Author(s), 2023, published in Optika Atmosfery i Okeana.

REMOTE SENSING OF ATMOSPHERE, HYDROSPHERE, AND UNDERLYING SURFACE

Air Composition over the Russian Arctic: 3—Trace Gases

O. Yu. Antokhina[a], P. N. Antokhin[a], V. G. Arshinova[a], M. Yu. Arshinov[a], G. Ancellet[b], B. D. Belan[a, *], S. B. Belan[a], D. K. Davydov[a], G. A. Ivlev[a], A. V. Kozlov[a], K. Law[b], P. Nédélec[c], T. M. Rasskazchikova[a], J.-D. Paris[d], D. E. Savkin[a], D. V. Simonenkov[a], T. K. Sklyadneva[a], G. N. Tolmachev[a], and A. V. Fofonov[a]

[a] *V.E. Zuev Institute of Atmospheric Optics, Siberian Branch, Russian Academy of Sciences, Tomsk, 634055 Russia*

[b] *Laboratoire Atmosphères, Milieux, Observations Spatiales LATMOS, UMR 8190, Paris, France*

[c] *Laboratoire d'Aerologie CNRS-UPS, Toulouse, France*

[d] *Laboratoire des Sciences du Climat et de l'Environnement, LSCE/IPSL, CNRS-CEA-UVSQ, Gif-sur-Yvette, France*

**e-mail: bbd@iao.ru*

Received July 21, 2022; revised September 5, 2022; accepted October 22, 2023

Abstract—Based on the results of a comprehensive experiment conducted in September 2020, the spatial distribution of the following trace gases over the seas of the Russian Arctic are analyzed: carbon monoxide (CO), ozone (O_3), nitrogen oxide and dioxide (NO and NO_2), and sulfur dioxide (SO_2). It is shown that the gas concentrations in the surface air layer over the seas (at an altitude of 200 m) vary in the range 18–36 ppb for O_3, 60–130 ppb for CO, 0.005–0.12 ppb for NO, 0.10–1.00 ppb for NO_2, and 0.06–0.80 ppb for SO_2. The distribution of the gases over the water area is heterogeneous over most seas, which most likely reflects differences in their uptake by the ocean and peculiarities of transport from the continent.

Keywords: Arctic, atmosphere, air, vertical distribution, nitrogen dioxide, sulfur dioxide, ozone, nitrogen oxide, carbon monoxide, transport, impurities, composition

DOI: 10.1134/S1024856023700057

INTRODUCTION

According to the Intergovernmental Panel on Climate Change (IPCC, IPCC), global warming is still ongoing, which is caused by changes in air composition due to increasing anthropogenic emissions of gases and aerosols [1]. This necessitates their monitoring in different regions of the globe, especially in regions where the warming is occurring faster, for example, the Arctic. There, the rate of increase in the air temperature was two to three times higher than in other regions of the Earth [2, 3], and according to the recent analysis results [4–6], it was four times higher. In this regard, the following questions naturally arise: how does warming in the Arctic affect the composition of the air [7–10] and how do pollutants arriving to the region affect the warming [11–14]? Answering them, as well as outlining an Arctic environmental preservation plan is possible only on the basis of measurements and analysis of direct and inverse connections between the climate warming and changes in air composition [15]. However, such data for the Russian Arctic are lacking.

Studies of the air composition in this region were carried out mainly in the surface air layer [16–18], in the near-water layer from drifting stations [19], and on board research vessels [20, 21]. Mainly greenhouse gases were measured [22]. Other trace atmospheric gases been poorly studied.

To fill the gap in data on the vertical distribution of gases and aerosols in air over the Russian Arctic, an experiment on sounding the atmosphere and water surface over the all seas of the Arctic Ocean from the Optik Tu-134 flying laboratory was performed in September 2020. The experiment and the equipment used are described and the average concentrations of atmospheric constituents over all seas are analyzed in [23]. In [24, 25], the methane and carbon dioxide distributions over each of the seas are analyzed. In this work, we analyze the distribution of the following trace gases over the seas of the Russian Arctic: carbon monoxide (CO), ozone (O_3), nitrogen oxide and dioxide (NO, NO_2), and sulfur dioxide (SO_2).

1. DATA AND METHODS

The list and specifications of the instruments used for the measurements are given in Table 1.

Gas concentration profiles were retrieved from measurements in the period indicated in Table 1 using a 15-point moving average and subsequent interpolation with an altitude step of 10 m. As is shown in [23], the differences in gas concentrations over different

Table 1. Specifications of gas analyzers

Model	Gas	Concentration range, ppm	Precision	Time constant, s
49C	O_3	0...200	±0.001 ppm	1
48C	CO	0...10000	<±1%	4
42*i*-TL	$NO/NO_2/NO_x$	0...0.5	±0.0004 ppm	10
43*i*-TLE	SO_2	0...20	±0.0002 ppm	10

seas are small above 5000 m. Therefore, in this work, we limit our analysis to this altitude.

2. VERTICAL DISTRIBUTION

2.1. Barents Sea and Coastal Areas

Survey over the Barents Sea was carried out from 12:58 to 15:39 on September 4, 2020. Here and below, we use the Greenwich Mean Time (GMT), because the experiment was carried out in several large administrative territories in nine time zones, where local and astronomical time do not coincide (for example, Yakutia).

Vertical distribution of the mixng ratios of trace gases from Table 1 measured over the Barents Sea are shown in Fig. 1, along with their vertical profiles measured over the coastal area upon departure from Arkhangelsk airport for comparison.

Tropospheric ozone is the fourth greenhouse gas to contribute to the net radiative forcing [26]. Our previous studies showed that in situ O_3 production in the lower atmosphere is insignificant in the Arctic regions [27, 28]. The experiment confirmed this conclusion (Fig. 1a). It can be seen that the concentration of O_3 in the surface air and the atmospheric boundary layer (ABL) sharply decreases compared to the higher tropospheric layers over all areas of the Barents Sea. Its mixing ratios are ≈50 ppb in the middle troposphere.

Since O_3 is a poorly soluble gas, unlike CO_2 [29], then the decrease in the O_3 concentration is explained not by its absorption by the ocean, but by the absence of its photochemical generation. In these areas, the main source of tropospheric O_3 is the stratosphere-to-troposphere transport (STT) [30]. Such low values at lower altitudes were possibly because of ozone depletion due to its chemical sink when interacting with bromine contained in marine aerosol [31].

Carbon monoxide concentration (Fig. 1b) varied over the Barents Sea within 60–120 ppb and its vertical distribution is close to neutral. One can note a slight increase in the CO concentration in the ABL over coastal areas. This altitude variation in CO indicates the absence of sources and sinks of this gas in this area. The measured values are lower than over continental areas [32, 33] and close to values characteristic of remote Antarctic regions [34]. Carbon monoxide, as well as NO, NO_2, NO_x, and SO_2, can be of both natural and anthropogenic origin [35]. Recent studies show that the concentrations of these compounds have sharply decreased in both urbanized and background regions [36, 37].

Nitric oxide content (Fig. 1c) fluctuated between 0.01–0.10 ppb over the Barents Sea, excluding the coastal area. In the Arkhangelsk region, its concentration increased to 0.24 ppb in the surface layer and up to 0.13 ppb in the ABL due to anthropogenic activity. The vertical distribution of NO and the variation in its concentrations are close to data [38, 39] for other regions of the Arctic.

Nitrogen dioxide has a slightly different vertical distribution over the Barents Sea (Fig. 1d). Its concentration, despite fluctuations, tends to decrease with altitude. Layers with high NO_2 content are visible in profiles *1*, *4*, and *5*, which is most likely due to transport from urbanized areas. On the day of measurements, air was advected from southwest [24, 25]. The NO_2 concentration over the sea was in the range 0.2–1.0 ppb; this is slightly higher than in [40] and lower than in [41].

Taking into account the rather low concentrations of nitrogen oxides over the Barents and all other seas under study, it is reasonable to consider data on these gases as estimates, without focusing on absolute values.

Sulfur dioxide concentrations over the Barents Sea were in the range 0.06–0.8 ppb (Fig. 1d) and were significantly lower than over coastal territories (it attained 2.7 ppb over Arkhangelsk). This points out to continental SO_2 sources and, apparently, anthropogenic. The data are in good agreement with the measurements of SO_2 vertical distribution over the Pacific Ocean [42] and are significantly lower than those obtained over continental China [43].

Figure 1e shows vertical profiles of NO_x over the Barents Sea. Since NO_x is the sum of NO and NO_2 and, as can be seen from Figs. 1c and 1d, NO_2 is almost an order of magnitude greater than NO in the case under study, this graph repeats the main features of Fig. 1d.

2.2. Kara Sea and Coastal Areas

Survey over the Kara Sea (Fig. 2) was carried out on September 6, 2020 [23, 24]. According to Fig. 2a, the O_3 concentration in the surface air layer and ABL sharply decreased over all areas of the Kara Sea compared to the upper tropospheric layers. In the middle troposphere, it ranged from 45 to 50 ppb. This range is narrower than over the Barents Sea. One can also note

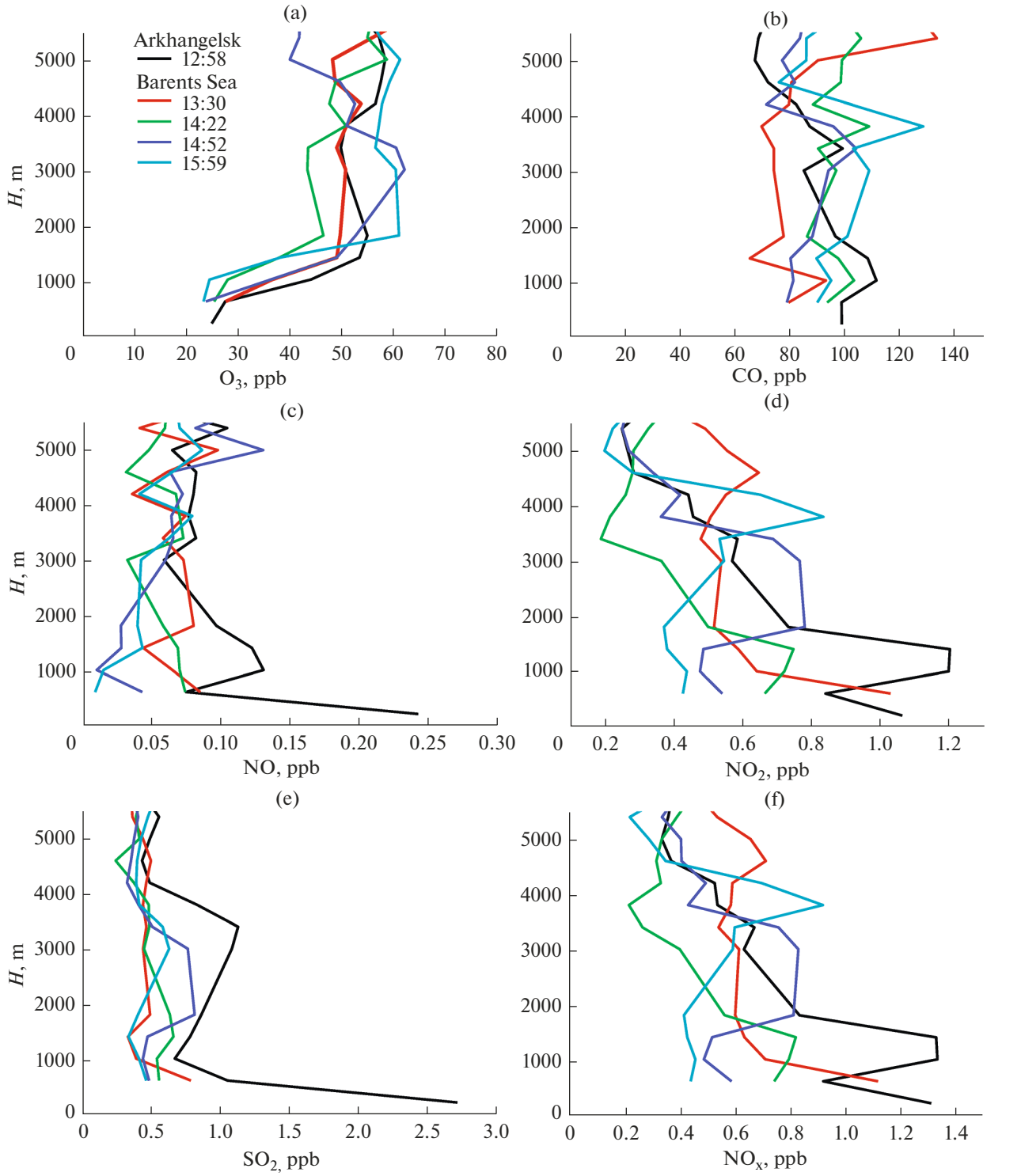

Fig. 1. Vertical distribution of concentrations of (a) O_3, (b) CO, (c) NO, (d) NO_2, (e) SO_2, and (f) NO_x over the Barents Sea on September 4, 2020.

a weak trend towards an increase in the O_3 concentration above the ABL.

Carbon monoxide concentration (Fig. 2b) varied within 60–130 ppb over the Kara Sea and decreased above the top of the ABL. One can also note its significant increase at an altitude of about 1000 m in the first profile measured over the water area (13:30). This altitude variation in the CO mixing ratio indicates the absence of sources and sinks of this gas in this area, but its transport from the continent. This is also supported

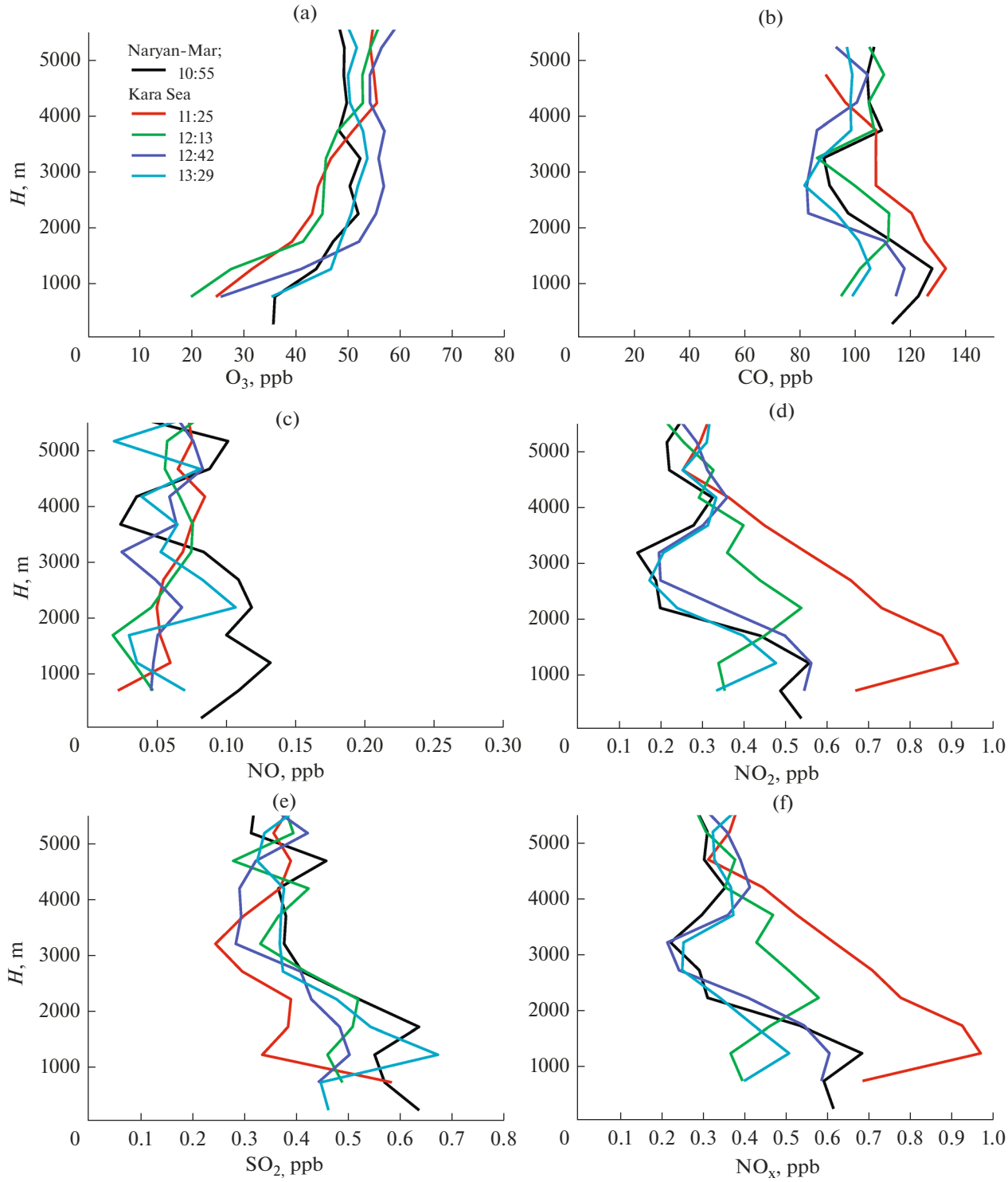

Fig. 2. Same as in Fig. 1, for the Kara Sea, September 6, 2020.

by higher CO concentrations over the Kara Sea compared to the Barents Sea.

Nitric oxide mixing ratios (Fig. 2c) over the Kara Sea, also excluding the coastal territory, fluctuated within 0.02–0.10 ppb. Near Naryan-Mar, its concentration increased to 0.13 ppb in the surface layer and up to 0.12 ppb in the ABL due to anthropogenic activity. The vertical distribution of NO is close to neutral with a slight tendency to increase with altitude. This points out to the absence of sources of this gas in the Kara Sea, and the increase in its content with altitude indicates transport from adjacent regions.

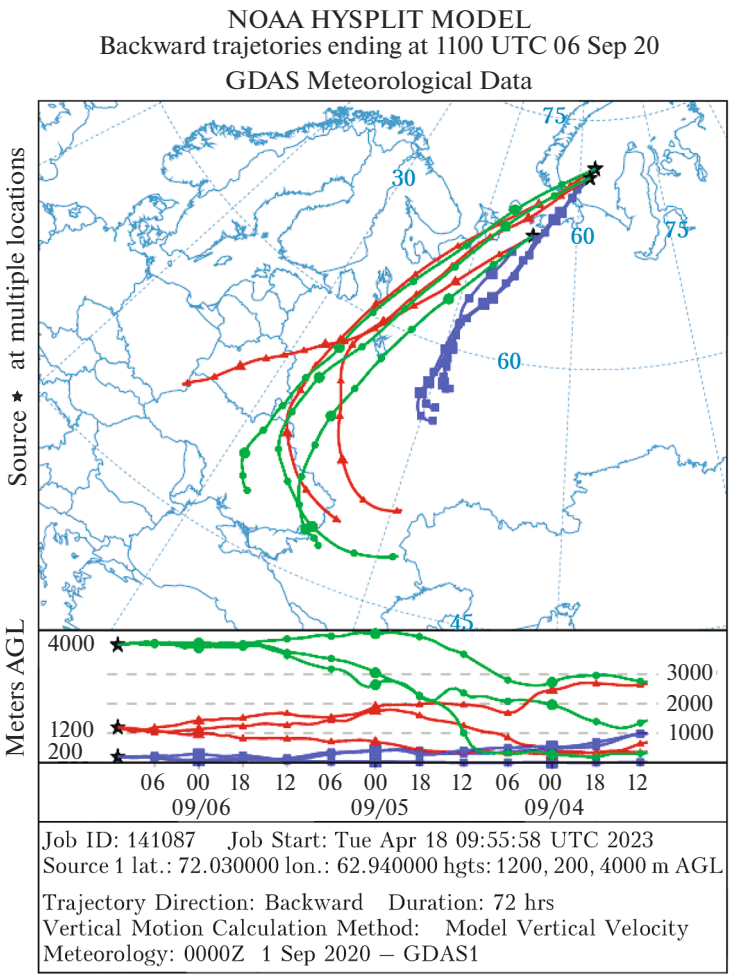

Fig. 3. Back trajectories of air masses for the Kara Sea and Naryan-Mar on September 6, 2020.

Vertical distribution of NO_2 over the Kara Sea is similar to that over the Barents Sea (Fig. 2d). Its concentration shows a trend to decrease with altitude, despite vertical fluctuations. Like for CO (Fig. 2b), the first profile measured over the water area (13:30) shows a layer with a high NO_2 content near 1000 m, which most likely reflects its transport from urbanized areas. The NO_2 concentration over the Kara Sea varied within 0.2–0.9 ppb, which is slightly less than over the Barents Sea.

Sulfur dioxide mixing ratio over the Kara Sea was in the range 0.25–0.66 ppb (Fig. 2d) and was comparable to the value over Naryan-Mar (0.64 ppb). This indicates the presence of weak SO_2 sources on land and over sea.

Figure 2f shows the vertical profiles of NO_x over the Kara Sea. Since NO_2 concentrations almost an order of magnitude greater than that of NO, then these curves repeat the main features of Fig. 2d.

To understand what caused the maximal CO and NO_2 concentrations at an altitude of about 1000 m, air mass backward trajectories were plotted in Fig. 3 for three altitudes above Naryan-Mar: 200, 1200 and 4000 m a.s.l. One can see that the air came from the same regions at most levels, except for one trajectory for the air mass with the maximal concentration of gases. This indicates origination of this air mass in western Europe. Taking into account the large number of industrial enterprises located there, we can assume that this maximum was caused by long-range transport of impurities.

2.3. Laptev Sea and Coastal Areas

Measurements over the Laptev Sea were carried out on September 9, 2020 (Fig. 4). The O_3 concentration in the surface air layer varied from 20 to 30 ppb and increased with altitude first quickly and then slower (Fig. 4a). Despite the large area under survey, the O_3 content slightly differed over different regions.

Carbon monoxide mixing ratios (Fig. 4b) ranged from 80 to 120 ppb and weakly varied with altitude over the Laptev Sea. Two profiles measured at the beginning of the flight over coastal areas (03:09) and at the end of the flight (05:58) show two CO concentra-

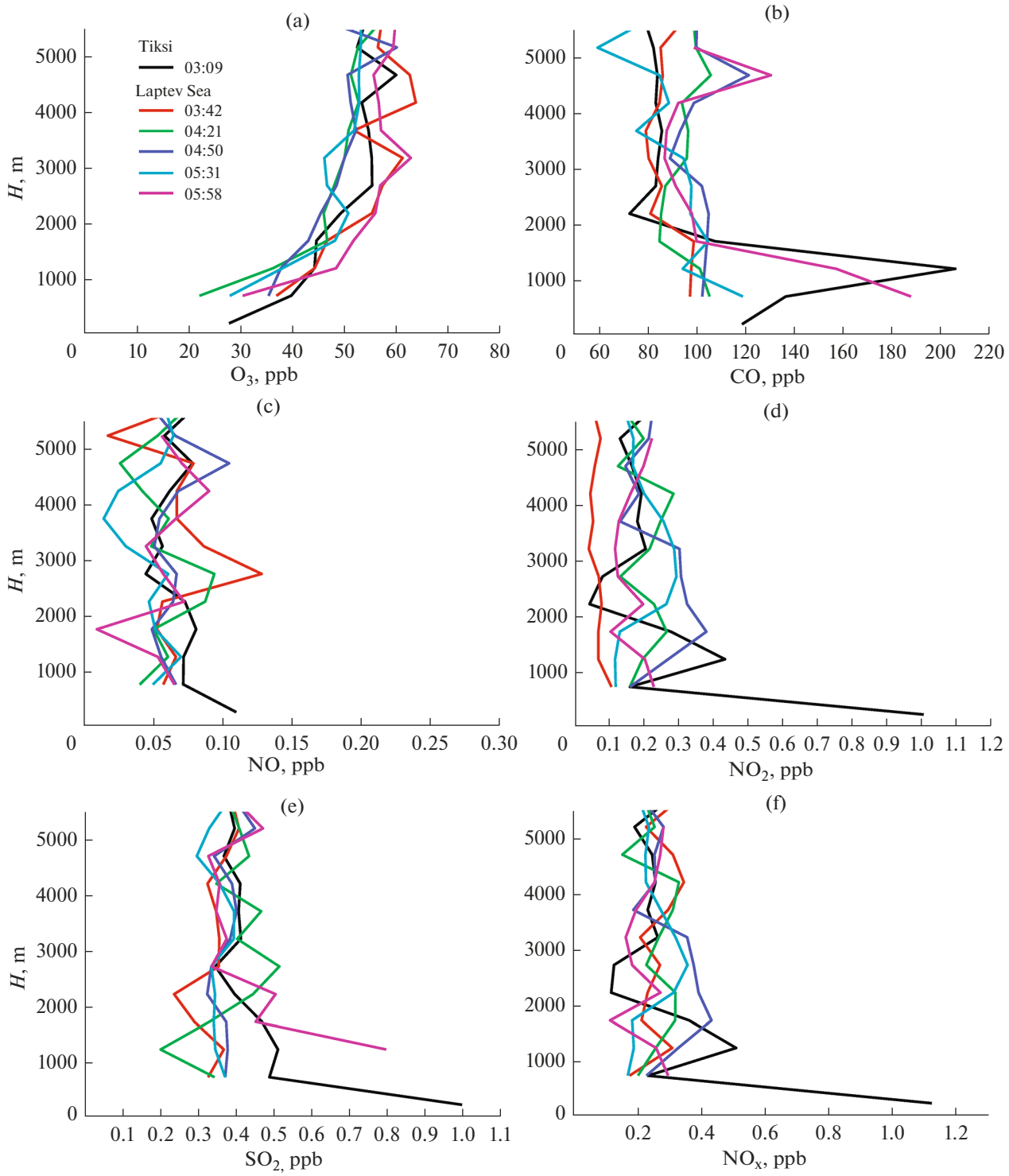

Fig. 4. Same as in Fig. 1, for the Laptev Sea, September 9, 2020.

tion maxima. Its neutral behavior in the free troposphere and the maxima in the ABL are possibly associated with air transport from the continent.

Nitric oxide concentration ranged from 0.005 to 0.10 ppb (Fig. 4c). Near Tiksi, it increased to 0.12 ppb in the surface air layer due to local anthropogenic activity. The vertical variation of the NO concentration is close to neutral. This indicates the absence of sources of this gas in the water area and its transfer from adjacent regions.

Vertical distribution of NO_2 over the Laptev Sea is not similar to the distributions over the Barents and

Kara seas (Figs. 2d and 4d). The altitude variation in the NO_2 concentration is almost neutral. Like for CO (Fig. 4b), the first profile measured over coastal areas (03:09) shows a layer with a high NO_2 mixing ratio near the water surface. The NO_2 concentration varied within 0.1–0.4 ppb over the Laptev Sea. This is comparable to the NO_2 dynamics over the Barents and Kara seas.

Sulfur dioxide concentration was in the range 0.2–0.5 ppb over the Laptev Sea (Fig. 4d). Like CO and NO_2, it increased (to 1.0 ppb) over coastal areas. This point out to were weak continental sources of SO_2.

Figure 4f shows the vertical profiles of NO_x over the Laptev Sea. Since the NO_2 content is almost an order of magnitude greater than that of NO, then Fig. 4f repeats the main features of Fig. 4d.

2.4. East Siberian Sea

The flight for surveying atmosphere over the water areas of the East Siberian and Chukchi seas was performed from Anadyr airport, which is located quite far from the Arctic Ocean. Therefore, the comparison between data obtained over the seas and the airport territory seems incorrect. The survey was conducted on September 15–16, 2020, taking into account the 12-hour difference with GMT. The measurement results are shown in Fig. 5.

The ozone distribution over the East Siberian Sea differs from the profiles measured over the seas located to the west (Fig. 5a). The difference between the O_3 concentrations in the surface air layer and the middle troposphere was lower; the ozone content in the middle troposphere decreased to 50 ppb; the differences between the O_3 concentrations in the lower troposphere in different water areas became smaller.

The CO concentration over different water areas varied from 85 to 120 ppb in the surface air layer and from 60 to 100 ppb in the middle troposphere. In Fig. 5b, the CO content trend to change with altitude is clearly seen.

Nitric oxide concentration also decreased over the East Siberian Sea (Fig. 5c) compared to the western seas. The vertical distribution of this gas shows negligible altitude variations. The NO content varied from 0.012 to 0.080 ppb from the surface air layer to the upper troposphere.

Mixing ratios of nitrogen and sulfur dioxides over the East Siberian Sea also insignificantly varied with altitude (Figs. 5d and 5e). The NO_2 concentration ranged from 0.1 to 0.38 ppb, and the SO_2 content varied within 0.3–0.5 ppb.

Vertical distribution of NO_x repeats NO_2 profiles.

2.5. Chukchi Sea

Airborne survey over the Chukchi Sea was carried out on September 15, 2020. The weather conditions are described in [23]. The measurement results are shown in Fig. 6. Here, like in Fig. 5, the vertical profile over coastal areas is not shown because it is far from the main sounding site.

The profile of O_3 over the Chukchi Sea significantly changed (Fig. 6a). The ABL, which was very low according to previous analysis [24, 25], is not shown here at all. The O_3 concentration in the surface air layer was in the range 28–32 ppb and almost uniformly increased to 60 ppb in the upper troposphere. This distribution is due to the change in the air mass transport direction to the Chukchi Sea. It was shown in [24, 25] that air came from the Asian part of the continent to the water areas of the western seas, while it came from the North America to the area under survey over the Chukchi Sea.

Apparently, the change in the direction of the main transport caused the abnormal CO distribution over the Chukchi Sea (Fig. 6b). Over three regions of the water area, it decreased above the ABL and then increased in the middle troposphere. Over the fourth region, it attained 118 ppb in the surface air layer and decreased to 74 ppb in the upper troposphere.

Nitrogen oxide slightly varied with altitude. Its concentrations were lower even then over the East Siberian Sea and ranged from 0.025 to 0.08 ppb.

The change in the air circulation in the region during the survey apparently resulted in changes in NO_2 and NO_x profiles (Figs. 6d and 6f). The concentration of these gases slightly decreased from the surface air layer to the middle troposphere and then significantly increased.

The sulfur dioxide concentration weakly changed with altitude and ranged from 0.25 to 0.52 ppb.

2.6. Bering Sea and Coastal Areas

Survey over the Bering Sea was carried out on September 16, 2020, immediately after the flight over the East Siberian Sea (Fig. 7). The purpose of that additional experiment was to verify features of the distributions of carbon dioxide and methane concentrations over the Chukchi and East Siberian Seas [24, 25].

Ozone profiles over land (03:38) and near the coast (04:48) (Fig. 7a) significantly differ, especially in the middle and upper troposphere. They show the intrusion of ozone from upper atmospheric layers. The other two profiles (04:24 and 05:21) are smoothed. Ozone concentration increases with altitude up to 70 ppb in the first two profiles and fluctuates within 20–25 ppb in the second pair of profile.

The CO content in the lower troposphere was close to that observed over the East Siberian and Chukchi Seas (Fig. 7b) and decreased with altitude.

The NO concentration with a smoothed vertical profile was slightly higher than over the East Siberian and Chukchi Seas (Fig. 7c).

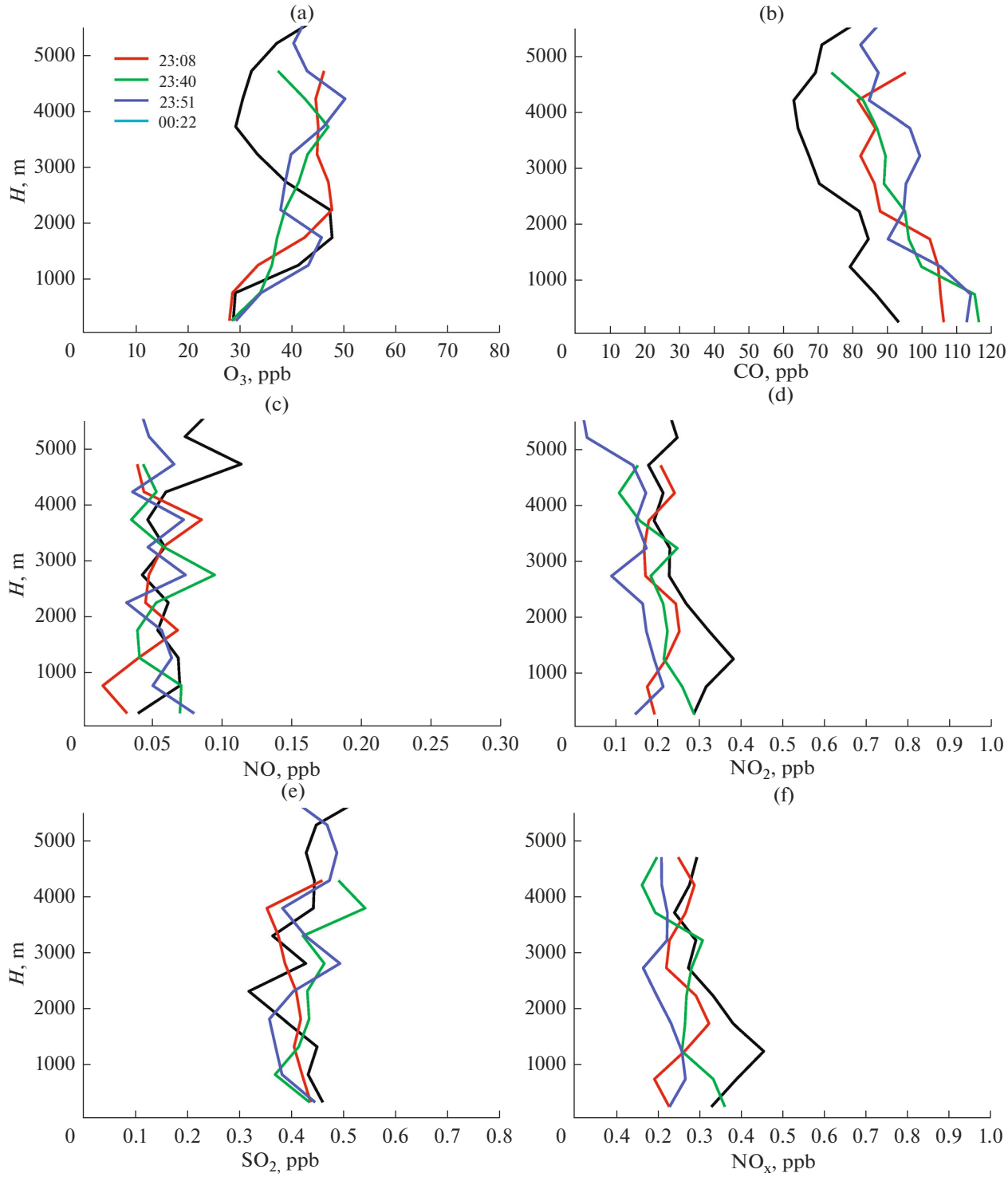

Fig. 5. Same as in Fig. 1, for the East Siberian Sea, September 15–16, 2020.

The concentrations of NO_2 and NO_x varied significantly over different areas of the Bering Sea (Figs. 7d and 7f). They were in the range 0.3–0.5 ppb over the coast and decreased to 0.012–0.28 ppb over the water area.

Sulfur dioxide concentration slightly varied with altitude, from 0.32 to 0.53 ppb.

Such differences between gas profiles over the Arctic seas and the Bering Sea are apparently explained by the peculiarities of air circulation during the experiment. If we refer to Fig. 8, it is easy to see that air to the regions of survey was transported from Alaska or along its coast, first to the Arctic and then to the region under study.

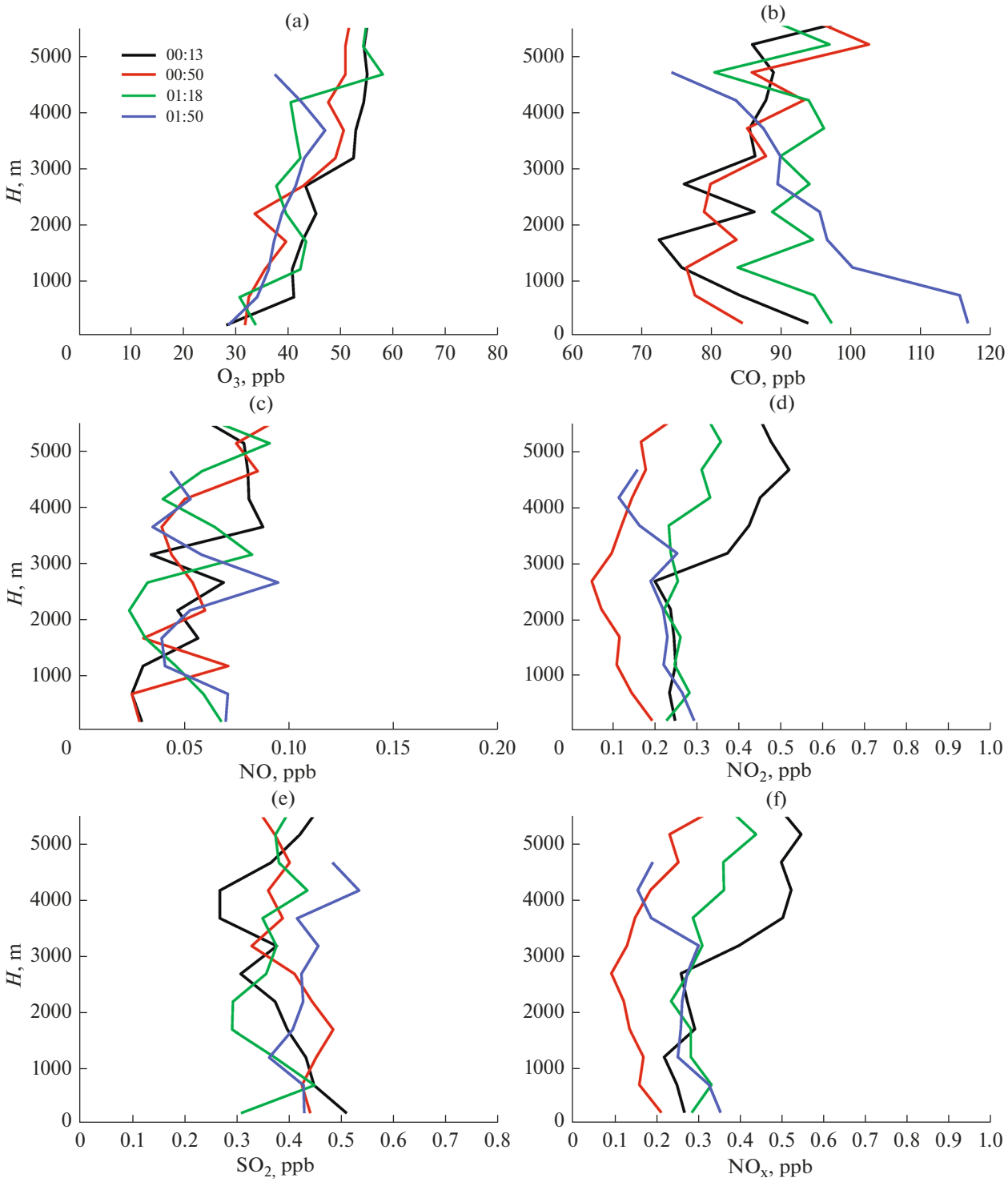

Fig. 6. Same as in Fig. 1, for the Chukchi Sea, September 15, 2020.

3. HORIZONTAL INHOMOGENEITIES IN DISTRIBUTION OF TRACE GASES

Horizontal inhomogeneities in the distribution of trace atmospheric gases over the Arctic seas were analyzed on the basis of data obtained during the flights performed at an altitude of 200 m. The concentrations of trace gases were recorded with a frequency of 1 or 0.1 Hz. The regions where the measurements were carried out are shown in Fig. 9. We assume that spatial heterogeneity of trace gas sources or sinks, if they exist on the ocean surface, should appear as concentration fluctuations at this altitude.

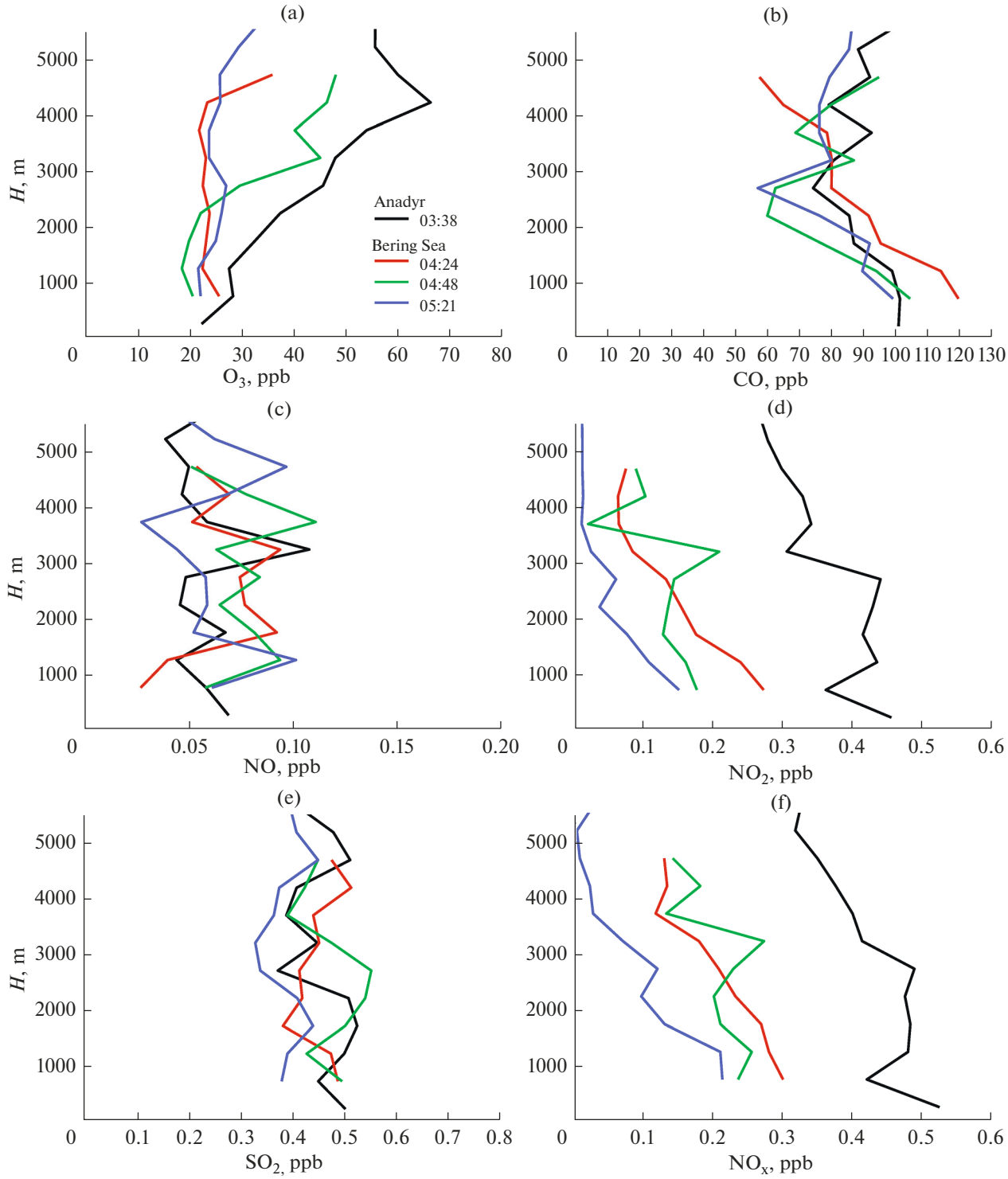

Fig. 7. Same as in Fig. 1, for the Bering Sea, September 16, 2020.

3.1. Ozone

During the experiment, two ozone analyzers of the same type operated on board the flying laboratory; they measured the O_3 concentration with a frequency of 1 and 0.4 Hz. The O_3 concentrations measured with a frequency of 1 Hz are shown in Fig. 10. The distribution of ozone mixing ratios over the water area was quite homogeneous only over the East Siberian Sea. Over other seas, it significantly changed when moving from one survey region to another. The variability of the

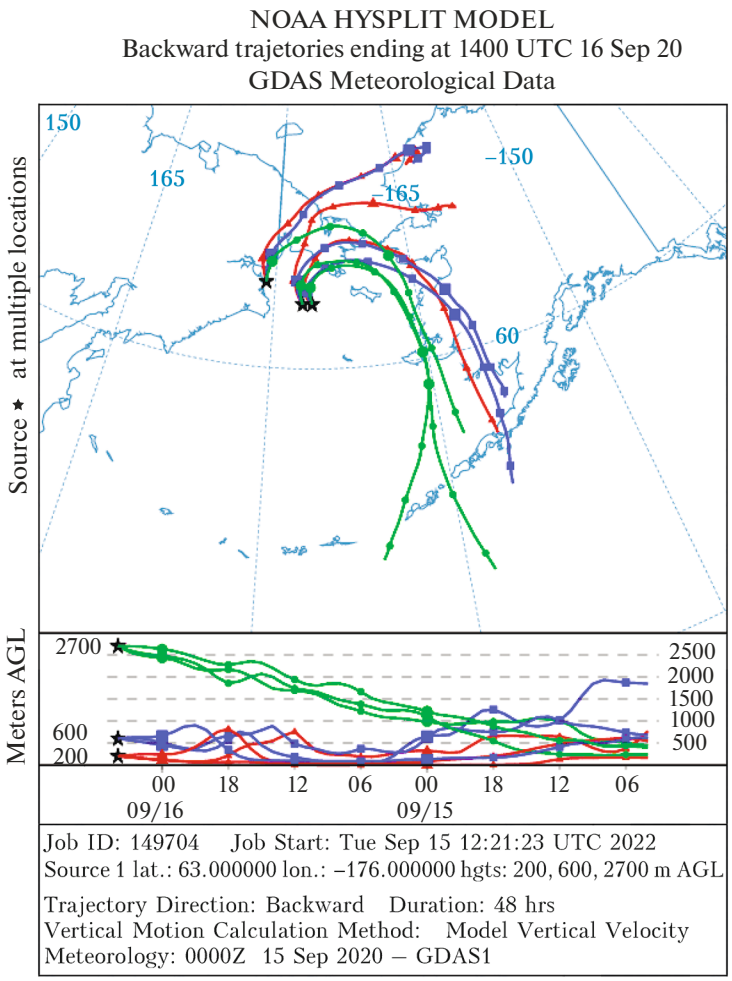

Fig. 8. Back trajectories of air masses for the Bering Sea on September 16, 2020.

O_3 concentration was maximal over the Laptev Sea (concentration difference was 15 ppb) and minimal over the East Siberian Sea (the difference was only 5 ppb).

Considering that ozone is not emitted by any source, but is produced in the troposphere or transferred from the stratosphere [44], such variability can only be explained by the heterogeneity of its transport from the continent.

3.2. Carbon Monoxide

This gas was also measured with a frequency of 1 Hz with gaps when the analyzer was automatically switched to a zero correction mode for 5 min after every 20 min of measurements (Fig. 11). One can see that the differences in CO concentrations over different regions of the seas were not as great as for O_3. The difference was also maximal (70 ppb) over the Laptev Sea and minimal (24 ppb) over the Chukchi Sea. The difference was from 40 to 50 ppb over other seas.

3.3. Nitric Oxide

Nitric oxide was measured at a frequency of 0.25 Hz. As a result, the period of recorded NO fluctuations is significantly shorter than for other gases measured at a frequency of 1 Hz (Fig. 12). It was shown that the NO concentration of nitric oxide was extremely low, 0.01–0.12 ppb, over all seas when being recorded at horizontal flight sections at an altitude of 200 m. Maximal values were recorded over the Barents, Kara, and Laptev Seas and minimal over the Chukchi and Bering Seas.

3.4. Nitrogen Dioxide

The NO_2 concentrations were maximal over the Barents Sea and lower over the Kara Sea (Fig. 13). Moreover, a large horizontal concentration gradient across the water area is clearly visible over the Barents Sea. The concentration of this gas decreased eastward and approached the detection limit of the analyzer.

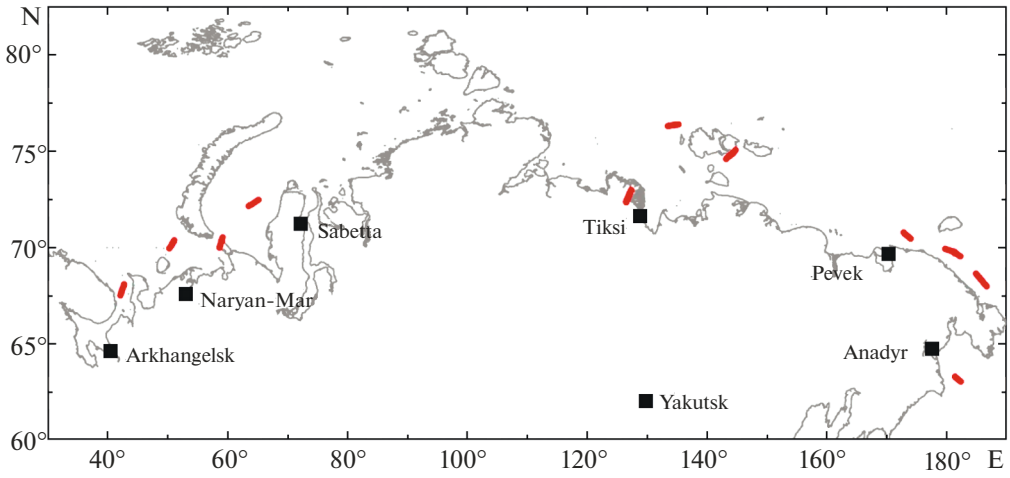

Fig. 9. Segments (red lines) of gas concentration measurements over the seas of the Russian Arctic and Pacific Ocean at an altitude of 200 m.

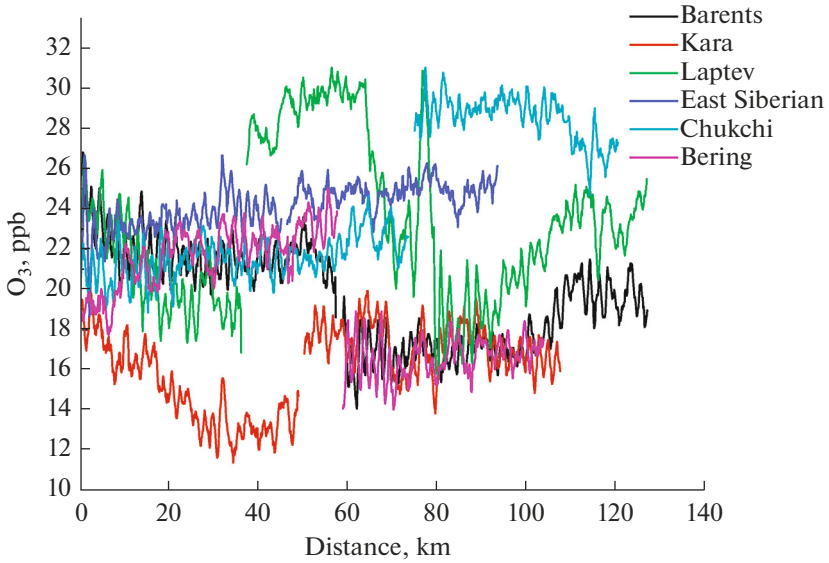

Fig. 10. Ozone concentration at an altitude of 200 m above the seas of the Russian Arctic and Pacific Ocean.

3.5. Sulfur Dioxide

The SO_2 distribution (Fig. 14) over the Arctic seas is very similar to NO_2. The difference between SO_2 concentrations over different seas is lower than for NO_2. Thus, the feature of a decrease in the concentration from west to east cannot be completely applied to SO_2.

4. RESULTS AND DISCUSSION

Let us compare the average concentrations of trace atmospheric gases over the seas under study. According to data in Table 2, concentrations of most gases show no clear trends to change from west to east, which was pronounced for CO_2 [25].

The lowest O_3 concentrations were recorded in the surface air layer (200–600 m) above the Barents, Kara, and Bering Seas. They were higher and almost identical over the Laptev, East Siberian, and Chukchi Seas. Since the air was transported to the Barents and Kara Seas from the continent, these values can be caused by sink of some ozone molecules due to reactions with other compounds advecting from the continent.

There is no clear trend in changes in the CO content as well. A slight increase in its values can be noted over the Kara, East Siberian, and Laptev Seas, the minimal value is over the Barents Sea. This is obviously due to the air advection from the continent to the water areas.

The NO content was extremely low in the Russian Arctic, in the range 0.03–0.07 ppb. This is the only gas with the concentration decreased from west to east, excluding the Bering Sea. The maximum was observed over the Barents Sea and the minimum over the Chukchi Sea.

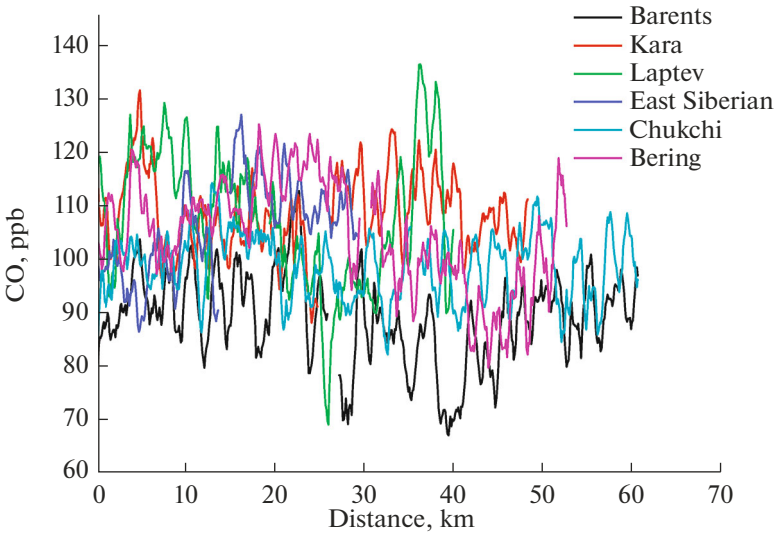

Fig. 11. Same as in Fig. 10, for carbon monoxide.

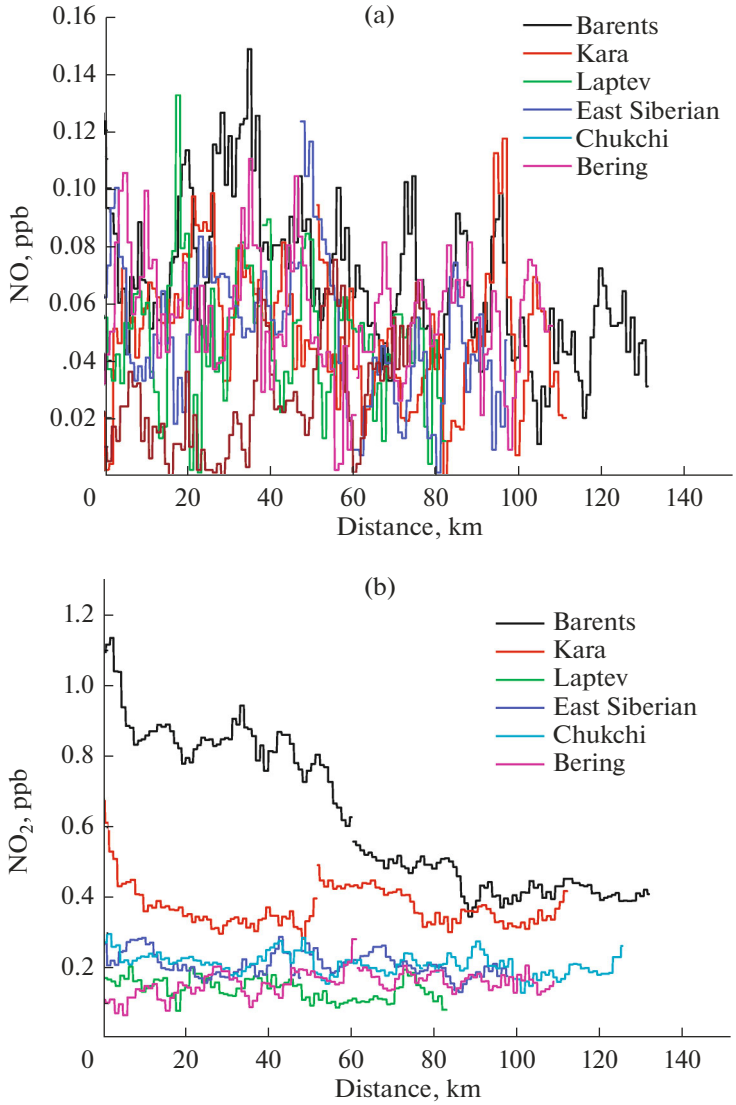

Fig. 12. Same as in Fig. 10, for nitric oxide.

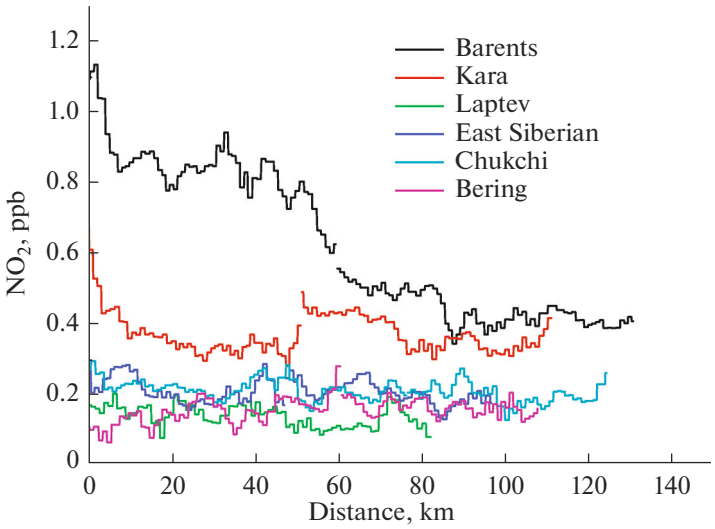

Fig. 13. Same as in Fig. 10, for nitrogen dioxide.

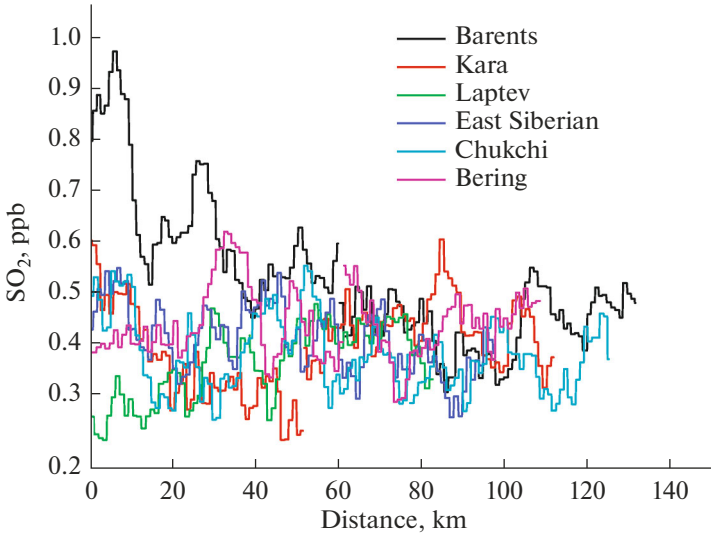

Fig. 14. Same as in Fig. 10, for sulfur dioxide.

The NO_2 concentration (although small in the Arctic region, but almost an order of magnitude higher than that of NO) also decreased from west to east, with the exception of the Laptev Sea. It is still difficult to explain why NO_2 content was the lowest over the Laptev Sea, though the concentration of its precursor (NO) is comparable with the neighboring seas. Differences in the NO and NO_2 concentrations determined the general dynamics of NO_x, which follows the behavior of NO_2.

The SO_2 content over the western seas is comparable to that of NO_x and even slightly higher than over the

Table 2. Average concentrations of trace atmospheric gases (ppb)

Gas	Sea					
	Barents	Kara	Laptev	East Siberian	Chukchi	Bering
O_3	19.6 ± 3.10	16.1 ± 2.60	23.3 ± 4.20	24.1 ± 2.10	24.3 ± 3.90	19.5 ± 3.40
CO	88.7 ± 14.8	107.8 ± 15.2	107.6 ± 18.8	105.4 ± 14.7	98.2 ± 12.9	104.4 ± 17.0
NO	0.07 ± 0.03	0.05 ± 0.02	0.05 ± 0.02	0.05 ± 0.02	0.03 ± 0.01	0.06 ± 0.02
NO	0.62 ± 0.21	0.37 ± 0.06	0.14 ± 0.03	0.21 ± 0.03	0.21 ± 0.03	0.16 ± 0.03
NO_x	0.69 ± 0.23	0.42 ± 0.05	0.19 ± 0.04	0.26 ± 0.04	0.24 ± 0.03	0.22 ± 0.03
SO_2	0.53 ± 0.14	0.40 ± 0.08	0.36 ± 0.07	0.41 ± 0.07	0.38 ± 0.07	0.44 ± 0.07

eastern seas. There are apparently weak sources of this gas in the eastern regions, which increase its background concentrations. This might well be caused by emissions from the Norilsk Nickel plant, which uses coal with a high sulfur content in some industrial processes.

The comparison of our data with similar data for the other regions of the Arctic shows that the O_3 and CO concentrations we obtained are comparable with the results of [45, 46]. The same low values of nitrogen oxides were recorded in [39, 40]. Studies of the vertical distribution of SO_2 concentration have not been carried out in recent years.

CONCLUSIONS

The comprehensive experiment on surveying the atmosphere for a quite short term made it possible to compare the concentrations of trace atmospheric gases over all the seas of the Russian Arctic and the Bering Sea in the Pacific Ocean. Their content, unlike of methane and carbon dioxide, was extremely low during the experiment.

The vertical distribution of ozone was characterized by an increase in its concentration with altitude. This indicates the weakness of in situ photochemical O_3 production and the predominance of ozone transport from the stratosphere. For other gases, either a decrease in their content with altitude or smoothed vertical profiles was observed. This indicates the absence of sources of these gases in the region or their low power.

For nitrogen and sulfur dioxides, a trend towards a decrease in their concentrations from west to east was found.

The areal distribution of the gases over most seas was heterogeneous. This most likely reflects differences in their absorption by the ocean and features of its transport from the continent.

It is important that the concentrations of all the measured gases were very low during the experiment, typical for remote background regions.

FUNDING

Airborne survey of the atmosphere was carried out with the Optik Tu-134 flying laboratory developed under the support of the Ministry of Science and Higher Education of the Russian Federation (V.E. Zuev Institute of Atmospheric Optics, Siberian Branch, Russian Academy of Sciences). Data processing and analysis of the results were also supported by the Ministry of Science and Higher Education of the Russian Federation (agreement no. 075-15-2021-934) within the project "Study of Anthropogenic and Natural Factors of Changes in the Air Composition and Environmental Objects in Siberia and the Russian Arctic under Conditions of Rapid Climate Change using the Optik Tu-134 flying laboratory."

CONFLICT OF INTEREST

The authors of this work declare that they have no conflicts of interest.

OPEN ACCESS

REFERENCES

1. "The summary for policymakers," in *Climate Change 2021: The Physical Science Basis. The Working Group I Contribution to the Sixth Assessment Report of the Intergovernmental Panel on Climate Change* (Cambridge University Press, Cambridge, 2021), pp. 1–41.
2. T. G. Shepherd, "Effects of a warming arctic," Science **353** (6303), 989–990 (2016).
3. M. R. Najafi, F. W. Zwiers, and N. P. Gillett, "Attribution of Arctic temperature change to grenhouse-gas and aerosol influences," Nat. Clim. Change, No. 2, 4 (2015).
4. M. Rantanen, A. Yu. Karpechko, A. Lipponen, K. Nording, O. Hyvarinen, K. Ruosteenoja, T. Vihma, and A. Laaksonen, "The Arctic has warmed nearly four times faster than the globe since 1979," Commun. Earth Environ. **3**, 168 (2022).
5. R. Thoman, M. L. Druckenmiller, and T. Moon, "State of the climate in 2021," Bull. Am. Meteorol. Soc. **103** (8), 257–S306 (2022).
6. M. Wendisch, M. Bruckner, S. Crewell, A. Ehrlich, J. Notholt, C. Lupkes, A. Macke, J. P. Burrows, A. Rinke, J. Quaas, M. Maturilli, V. Schemann, M. D. Shupe, E. F. Akansu, C. Barrientos-Velasco, K. Barfuss, A.-M. Blechschmidt, K. Block, I. Bougoudis, H. Bozem, C. Bockmann, A. Bracher, H. Bresson, L. Bretschneider, M. Buschmann, D. G. Chechin, J. Chylik, S. Dahlke, H. Deneke, K. Dethloff, T. Donth, W. Dorn, R. Dupuy, K. Ebell, U. Egerer, R. Engelmann, O. Eppers, R. Gerdes, R. Gierens, I. V. Gorodetskaya, M. Gottschalk, H. Griesche, V. M. Gryanik, D. Handorf, B. Harm-Altstadter, J. Hartmann, M. Hartmann, B. Heinold, A. Herber, H. Herrmann, G. Heygster, I. Hoschel, Z. Hofmann, J. Holemann, A. Hunerbein, S. Jafariserajehlou, E. Jakel, C. Jacobi, M. Janout, F. Jansen, O. Jourdan, Z. Juranyi, H. Kalesse-Los, T. Kanzow, R. Kathner, L. L. Kliesch, M. Klingebiel, E. M. Knudsen, T. Kovacs, W. Kortke, D. Krampe, J. Kretzschmar, D. Kreyling, B. Kulla, D. Kunkel, A. Lampert, M. Lauer, L. Lelli, A. von Lerber, O. Linke, U. Lohnert, M. Lonardi, S. N. Losa,

M. Losch, M. Maahn, M. Mech, L. Mei, S. Mertes, E. Metzner, D. Mewes, J. Michaelis, G. Mioche, M. Moser, K. Nakoudi, R. Neggers, R. Neuber, T. Nomokonova, J. Oelker, I. Papakonstantinou-Presvelou, F. Patzold, V. Pefanis, C. Pohl, M. van Pinxteren, A. Radovan, M. Rhein, M. Rex, A. Richter, N. Risse, C. Ritter, P. Rostosky, V. V. Rozanov, DonosoE. Ruiz, GarfiasP. S. Saavedra, M. Salzmann, J. Schacht, M. Schafer, J. Schneider, N. Schnierstein, P. Seifert, S. Seo, H. Siebert, M. A. Soppa, G. Spreen, I. S. Stachlewska, J. Stapf, F. Stratmann, I. Tegen, C. Viceto, C. Voigt, M. Vountas, A. Walbrol, M. Walter, B. Wehner, H. Wex, S. Willmes, M. Zanatta, and S. Zeppenfeld, "Atmospheric and surface processes, and feedback mechanisms determining Arctic amplification," Bull. Am. Meteorol. Soc. **104** (1), E208–E242 (2023).

7. M. R. Najafi, F. W. Zwiers, and N. P. Gillett, "Attribution of Arctic temperature change to grenhouse-gas and aerosol influences," Nature Clim. Change, No. 2, 4 (2015).
8. M. Sand, T. K. Berntsen, K. von Salzen, M. G. Flanner, J. Langner, and D. G. Victor, "Response of Arctic temperature to changes in emissions of short-lived climate forcers," Nat. Clim. Change, No. 11, 4 (2015).
9. D. Nomura, M. A. Granskog, A. Fransson, M. Chierici, A. Silyakova, K. I. Ohshima, L. Cohen, B. Delille, S. R. Hudson, and G. S. Dieckmann, "CO_2 flux over young and snow-covered Arctic pack ice in winter and spring," Biogeosci. **15** (11), 3331–3343 (2018).
10. M. D. Willis, R. W. Leaitch, and J. P. D. Abbatt, "Processes controlling the composition and abundance of Arctic aerosol," Rev. Geophys. **56** (4), 621–671 (2018).
11. S. R. Arnold, K. S. Law, C. A. Brock, J. L. Thomas, S. M. Starkweather, K. Salzen, A. Stohl, S. Sharma, M. T. Lund, M. G. Flanner, T. Petaja, H. Tanimoto, J. Gamble, J. E. Dibb, M. Melamed, N. Johnson, M. Fider, V.-P. Tynkkynen, A. Baklanov, S. Eckhardt, S. A. Monks, J. Browse, and H. Bozem, "Arctic air pollution: Challenges and opportunities for the next decade," Elem. Sci. Anth., No. 4, 16 (2016).
12. K. S. Law, A. Stohl, P. K. Quinn, C. A. Brock, J. F. Burkhart, J. D. Paris, G. Ancellet, B. Singh, A. Roiger, and H. Schlager, "Arctic air pollution," Bull. Am. Meteorol. Soc. **95** (12), 1873–1895 (2014).
13. A. Roiger, J.-L. Thomas, H. Schlager, K. S. Law, J. Kim, A. Schafler, B. Weinzierl, F. Dahlkotter, I. Krisch, L. Marelle, A. Minikin, J.-C. Raut, A. Reiter, M. Rose, M. Scheibe, P. Stock, R. Baumann, C. Clerbaux, M. George, T. Onishi, and J. Flemming, "Quantifying emerging local anthropogenic emissions in the Arctic region," Bull. Am. Meteorol. Soc. **96** (3), 441–460 (2015).
14. N. Evangeliou, Y. Balkanski, W. M. Hao, A. Petkov, R. P. Silverstein, R. Corley, B, Nordgren, S. P. Urbanski, S. Eckhardt, A. Stohl, P. Tunved, S. Crepinsek, A. Jefferson, S. Sharma, J. K. Njgaard, and H. Skov, "Wildfires in Northern Eurasia affect the budget of black carbon in the Arctic—a 12-year retrospective synopsis (2002–2013)," Atmos. Chem. Phys. **16** (12), 7587–7604 (2016).
15. M. Kulmala, T. Nieminen, R. Chellapermal, R. Makkonen, J. Back, and V.-M. Kerminen, "Climate feedbacks linking the increasing atmospheric CO_2 concentration, BVOC emissions, aerosols and clouds in forest ecosystems," in *Biology, Controls and Model Tree Volatile Organic Compound Emissions,* Ed. by U. Niinemets and R.K. Monson (Springer, Dordrecht, 2010).
16. S. Tei, T. Morozumi, A. Kotani, S. Takano, A. Sugimoto, S. Miyazaki, R. Shingubara, R. Fan, R. Petrov, E. Starostin, R. Shakhmatov, A. Nogovitcyn, and T. Maximov, "Seasonal variations in carbon dioxide exchange fluxes at a taiga-tundra boundary ecosystem in northeastern Siberia," Polar Sci. **28**, 100644 (2021).
17. S. Juutinen, M. Aurela, J.-P. Tuovinen, V. Ivakhov, M. Linkosalmi, A. Rasanen, T. Virtanen, J. Mikola, J. Nyman, E. Vaha, M. Loskutova, A. Makshtas, and T. Laurila, "Variation in CO_2 and CH_4 fluxes among land cover types in heterogeneous Arctic tundra in northeastern Siberia," Biogeosci. **19** (13), 3151–3167 (2022).
18. V. M. Ivakhov, N. N. Paramonova, V. I. Privalov, A. V. Zinchenko, M. A. Loskutova, A. P. Makshtas, V. Yu. Kustov, T. Laurila, M. Aurela, and E. Asmi, "Atmospheric concentration of carbon dioxide at Tiksi and Cape Baranov stations in 2010–2017," Russ. Meteorol. Hydrol. **44** (4), 291–299 (2019).
19. A. P. Nagurnyi, "Analysis of measurement data on carbon dioxide concentration in the near-ice surface atmosphere at North Pole-35 drifting ice station (2007–2008)," Russ. Meteorol. Hydrol. **35** (9), 619–623 (2010).
20. I. I. Pipko, S. P. Pugach, and I. P. Semiletov, "CO_2 dynamics on the shelf of the East Siberian Sea," Russ. Meteorol. Hydrol. **35** (9), 624–632 (2010).
21. I. P. Semiletov, N. E. Shakhova, I. I. Pipko, S. P. Pugach, A. N. Charkin, O. V. Dudarev, D. A. Kosmach, and S. Nishino, "Space-time dynamics of carbon and environmental parameters related to carbon dioxide emissions in the Buor-Khaya Bay and adjacent part of Laptev Sea," Biogeosci. **10** (9), 5977–5996 (2013).
22. A. V. Klepikov and A. I. Danilov, "Results of Russian studies of polar meteorology in 2015–2018," Izv., Atmos. Ocean. Phys. **57** (3), 233–246 (2021).
23. B. D. Belan, G. Ancellet, I. S. Andreeva, P. N. Antokhin, V. G. Arshinova, M. Y. Arshinov, Y. S. Balin, V. E. Barsuk, S. B. Belan, D. G. Chernov, D. K. Davydov, A. V. Fofonov, G. A. Ivlev, S. N. Kotel'nikov, A. S. Kozlov, A. V. Kozlov, K. Law, A. V. Mikhal'chishin, I. A. Moseikin, S. V. Nasonov, P. Nedelec, O. V. Okhlopkova, S. E. Ol'kin, M. V. Panchenko, J.-D. Paris, I. E. Penner, I. V. Ptashnik, T. M. Rasskazchikova, I. K. Reznikova, O. A. Romanovskii, A. S. Safatov, D. E. Savkin, D. V. Simonenkov, T. K. Sklyadneva, G. N. Tolmachev, S. V. Yakovlev, and P. N. Zenkova, "Integrated airborne investigation of the air composition over the Russian sector of the Arctic," Atmos. Meas. Tech. **15** (13), 3941–3967 (2022).
24. O. Yu. Antokhina, P. N. Antokhin, V. G. Arshinova, M. Yu. Arshinov, B. D. Belan, S. B. Belan, E. V. Gurulev, D. K. Davydov, G. A. Ivlev, A. V. Kozlov, K. Law, P. Nedelec, T. M. Rasskazchikova, J.-D. Paris, D. E. Savkin, D. V. Simonenkov, T. K. Sklyadneva, G. N. Tolmachev, and A. V. Fofonov, "Air composition over the Russian Arctic: 1—Methane," Atmos. Ocean. Opt. **36** (5), 470–489 (2023).
25. O. Yu. Antokhina, P. N. Antokhin, V. G. Arshinova, M. Yu. Arshinov, B. D. Belan, S. B. Belan, E. V. Gurulev, D. K. Davydov, G. A. Ivlev, A. V. Kozlov, K. Law, P. Nedelec, T. M. Rasskazchikova, J.-D. Paris, D. E. Savkin, D. V. Simonenkov, T. K. Sklyadneva, G. N. Tolmachev, and A. V. Fofonov, "Air composition over the Russian Arctic: 2—Carbon dioxide," Atmos. Ocean. Opt. **36** (5), 490–500 (2023).

26. M. J. Rowlinson, A. Rap, D. S. Hamilton, R. J. Pope, S. Hantson, S. R. Arnold, J. O. Kaplan, A. Arneth, M. P. Chipperfield, P. M. Forster, and L. Nieradzik, "Tropospheric ozone radiative forcing uncertainty due to pre-industrial fire and biogenic emissions," Atmos. Chem. Phys. **20** (18), 10937–10951 (2020).
27. P. N. Antokhin, V. G. Arshinova, M. Yu. Arshinov, B. D. Belan, S. B. Belan, D. K. Davydov, G. A. Ivlev, A. V. Kozlov, F. Nedelek, J.-D. Parizh, T. M. Rasskazchikova, D. E. Savkin, D. V. Simonenkov, T. K. Sklyadneva, G. N. Tolmachev, and A. V. Fofonov, "Large-scale studies of gaseous and aerosol composition of air over Siberia," Opt. Atmos. Okeana **27** (3), 232–239 (2014).
28. O. Yu. Antokhina, P. N. Antokhin, V. G. Arshinova, M. Yu. Arshinov, B. D. Belan, S. B. Belan, D. K. Davydov, G. A. Ivlev, A. V. Kozlov, P. Nedelec, J.-D. Paris, T. M. Rasskazchikova, D. E. Savkin, D. V. Simonenkov, T. K. Sklyadneva, G. N. Tolmachev, and A. V. Fofonov, "Vertical distributions of gaseous and aerosol admixtures in air over the Russian Arctic," Atmos. Ocean. Opt. **31** (3), 300–310 (2018).
29. N. L. Glinka, *Cloud Chemistry* (Khimiya, Leningrad, 1985) [in Russian].
30. P. N. Antokhin and B. D. Belan, "Control of the dynamics of tropospheric ozone through the stratosphere," Atmos. Ocean. Opt. **26** (3), 207–213 (2013).
31. L. Cao, S. Li, Y. Gu, and Y. Luo, "A three-dimensional simulation and process analysis of tropospheric ozone depletion events (ODEs) during the springtime in the Arctic using CMAQ (Community Multiscale Air Quality Modeling System)," Atmos. Chem. Phys. **23** (5), 3363–3382 (2023).
32. D. K. Davydov, B. D. Belan, P. N. Antokhin, O. Yu. Antokhina, V. V. Antonovich, V. G. Arshinova, M. Yu. Arshinov, A. Yu. Akhlestin, S. B. Belan, N. V. Dudorova, G. A. Ivlev, A. V. Kozlov, D. A. Pestunov, T. M. Rasskazchikova, D. E. Savkin, D. V. Simonenkov, T. K. Sklyadneva, G. N. Tolmachev, A. Z. Fazliev, and A. V. Fofonov, "Monitoring of atmospheric parameters: 25 years of the Tropospheric Ozone Research station of the Institute of Atmospheric Optics, Siberian Branch, Russian Academy of Sciences," Atmos. Ocean. Opt. **32** (2), 180–192 (2019).
33. Yu. A. Shtabkin, K. B. Moiseenko, A. I. Skorokhod, A. V. Vasil'eva, and M. Heimann, "Sources of and variations in tropospheric CO in central Siberia: numerical experiments and observations at the Zotino Tall Tower Observatory," Izv., Atmos. Ocean. Phys. **52** (1), 45–56 (2016).
34. V. P. Ustinov, E. L. Baranova, K. N. Visheratin, M. I. Grachev, and A. V. Kalsin, "Variations of carbon monoxide in the atmosphere of Antarctica according to ground-based and satellite measurements," Issled. Zemli Kosmosa, No. **2**, 97–100 (2019).
35. J. H. Seinfeld and S. N. Pandis, *Chemistry and Physics: From air Pollution to Climate Change* (Wiley, New Jersey, 2006).
36. A. S. Lefohn, J. D. Husar, and R. B. Husar, "Estimating historical anthropogenic global sulfur emission patterns for the period 1850–1990," Atmos. Environ. **33** (21), 3435–3444 (1999).
37. J. N. Galloway, W. Winiwarter, A. Leip, A. M. Leach, A. Bleeker, and J. W. Erisman, "Nitrogen footprints: Past, present and future," Environ. Res. Lett. **9115003**, 11 (2014).
38. J. R. Olson, J. H. Crawford, B. Brune, J. Mao, X. Ren, A. Fried, B. Anderson, E. Apel, M. Beaver, D. Blake, G. Chen, J. Crounse, J. Dibb, G. Diskin, S. R. Hall, L. G. Huey, D. Knapp, D. Richter, D. Riemer, J. St. Clair, K. Ullmann, J. Walega, P. Weibring, A. Weinheimer, P. Wennberg, and A. Wisthaler, "An analysis of fast photochemistry over high northern latitudes during spring and summer using in-situ observations from ARCTAS and TOPSE," Atmos. Chem. Phys. **12** (15), 6799–6825 (2012).
39. A. Ianniello, R. Salzano, R. Salvatori, G. Esposito, F. Spataro, M. Montagnoli, R. Mabilia, and A. Pasini, "Nitrogen oxides (NO_x) in the Arctic troposphere at Ny-Alesund (Svalbard Islands): Effects of anthropogenic pollution sources," Atmosphere **12** (7), 901 (2021).
40. V. Shah, D. J. Jacob, R. Dang, L. N. Lamsal, S. A. Strode, S. D. Steenrod, K. F. Boersma, S. D. Eastham, T. M. Fritz, Ch. Thompson, J. Peischl, I. Bourgeois, I. B. Pollack, B. A. Nault, R. C. Cohen, P. Campuzano-Jost, J. L. Jimenez, S. T. Andersen, L. J. Carpenter, T. Sherwen, and M. J. Evans, "Nitrogen oxides in the free troposphere: Implications for tropospheric oxidants and the interpretation of satellite NO_2 measurements," Atmos. Chem. Phys. **23** (2), 1227–1257 (2023).
41. L. N. Lamsal, S. J. Janz, N. A. Krotkov, K. E. Pickering, R. J. D. Spurr, M. G. Kowalewski, C. P. Loughner, J. H. Crawford, W. H. Swartz, and J. R. Herman, "High-resolution NO_2 observations from the airborne compact atmospheric mapper: Retrieval and validation," J. Geophys. Res.: Atmos. **122** (3), 1953–1970 (2017).
42. F. H. Tu, D. C. Thornton, A. R. Bandy, G. R. Carmichael, Y. Tang, K. L. Thornhill, G. W. Sachse, and D. R. Blake, "Long-range transport of sulfur dioxide in the Central Pacific," J. Geophys. Res. **109**, 08 (2004).
43. Li. Can, J. W. Stehr, L. T. Marufu, Z. Li, and R. R. Dickerson, "Aircraft measurements of SO_2 and aerosols over Northeastern China: Vertical profiles and the influence of weather on air quality," Atmos. Environ. **62**, 492–501 (2012).
44. B. D. Belan and T. K. Sklyadneva, "Tropospheric ozone. 4. Photochemical formation of tropospheric ozone: The role of solar radiation," Atmos. Ocean. Opt. **21** (10), 746–754 (2008).
45. C. H. Whaley, K. S. Law, J. L. Hjorth, H. Skov, S. R. Arnold, J. Langner, J. B. Pernov, G. Bergeron, I. Bourgeois, J. H. Christensen, R.-Y. Chien, M. Deushi, X. Dong, P. Effertz, G. Faluvegi, M. Flanner, J. S. Fu, M. Gauss, G. Huey, U. Im, R. Kivi, L. Marelle, T. Onishi, N. Oshima, I. Petropavlovskikh, J. Peischl, D. A. Plummer, L. Pozzoli, J.-C. Raut, T. Ryerson, R. Skeie, S. Solberg, M. A. Thomas, C. Thompson, K. Tsigaridis, S. Tsyro, S. T. Turnock, K. von Salzen, andD. W. Tarasick, "Arctic tropospheric ozone: Assessment of current knowledge and model performance," Atmos. Chem. Phys. **23** (1), 637–661 (2023).
46. A. Dekhtyareva, M. Hermanson, A. Nikulina, O. Hermansen, T. Svendby, K. Holmen, and R. G. Graversen, "Springtime nitrogen oxides and tropospheric ozone in Svalbard: Results from the measurement station network," Atmos. Chem. Phys. **22** (17), 11631–11656 (2022).